metals

Article

Mechanical Properties Improvement of Laser Tailor Welded Blanks of DP600 Steel by Magnetic Treatment

Yanli Song [1,2,3,*], Cheng Yu [1,2,3], Hailong Yu [3] and Chenyu Zhao [3]

1 Hubei Key Laboratory of Advanced Technology of Automotive Parts, Wuhan University of Technology, Wuhan 430070, China; 1015045671@whut.edu.cn
2 Hubei Collaborative Innovation Center for Automotive Components Technology, Wuhan University of Technology, Wuhan 430070, China
3 School of Automotive Engineering, Wuhan University of Technology, Wuhan 430070, China; yuhailong@gaei.cn (H.Y.); 13250704923@163.com (C.Z.)
* Correspondence: ylsong@whut.edu.cn; Tel.: +86-155-2751-0094

Academic Editor: Ian Baker
Received: 6 February 2017; Accepted: 28 February 2017; Published: 8 March 2017

Abstract: The influence of magnetic treatment on the yield strength, the ultimate tensile strength and the elongation of laser tailor welded blanks (TWBs) of DP600 steel was investigated by uniaxial tensile tests. The experimental results showed that the yield strength and the ultimate tensile strength of the TWBs had only a slight change, but the elongation increased by 13.90%–36.23% after the magnetic treatment. The dislocation distributions in the fusion zone (FZ) and the heat-affected zone (HAZ) were observed respectively by transmission electron microscopy (TEM). It was found that after magnetic treatment, the dislocations in both the FZ and the HAZ of the TWBs increased and showed a relatively uniform distribution. The mechanism of the mechanical property improvement of the TWBs by the magnetic treatment was then revealed on the basis of the relationship model between the dislocation and shear strain, considering the evolution of magnetic domains and Frank-Read dislocation multiplication in a magnetic field.

Keywords: mechanical properties; magnetic treatment; laser tailor welded blanks; dislocations

1. Introduction

Tailor welded blanks (TWBs) are made up of several steels with different materials, thicknesses and/or coatings to meet the diverse requirements of the components on the properties and thickness of the material [1]. Compared to other welding methods, laser welding can create a narrow fusion zone (FZ) and heat-affected zone (HAZ), and has become a widely used welding method of TWBs in the modern automobile industry [2,3]. However, the performance of laser TWBs is greatly reduced due to the existence of welded joints, which limits their application in automobiles [4–8]. Farabi [9] researched the tensile properties of laser TWBs of DP600 steel and the results showed that the hardness increased significantly in the FZ, the yield strength increased and the ultimate tensile strength remained almost unchanged after welding. Kang [10] investigated the mechanical properties and formability of laser-welded 600 MPa grade TRIP (Transformation Induced Plasticity) steel and DP (Dual Phase) steel and the results showed that the FZ hardness increased, the yield strength and ultimate tensile strength increased, but the elongation and the formability decreased. Therefore, it is important to find approaches to improve the ductility of TWBs, especially for those made of high-strength steels.

Magnetic treatment is an advanced method used to improve the mechanical properties of metallic materials [11]. At present, many scientific studies are being carried out to explore the rules and mechanisms of magnetic treatment. Zhao [12] detected the micro-hardness of high-speed steel for cutting tools under a pulsed magnetic field, and found that magnetic treatment with appropriate parameters clearly improved the micro-hardness of the high-speed steel. Celik [13] investigated the fatigue life of AISI 4140 steel under different magnetic field intensities and found that the fatigue life increased when the magnetic field was applied up to 30% of the fatigue fracture cycle of the untreated samples, and the treated effects also varied according to different magnetic field intensities. Klamechi [14] researched the residual stress of curved strip samples with and without applying an external magnetic field and the results showed that the residual stress was reduced by 4%–13% after the particular pulsed magnetic treatment. Cai [15] studied the effects of the magnetic field intensity orientation on the welding residual stress release by the pulsed magnetic field treatment and the results showed that the welding residual stress was reduced by up to 26% when the magnetic field was oriented along the blank thickness. Song [16] investigated the welding residual stress in low-alloy steel with a low-frequency alternating magnetic treatment and the experimental results revealed that the welding residual stress was reduced by 20%–24%.

Besides the aforementioned welding residual stress relief caused by magnetic treatment, other changes in the microstructures and properties of TWBs under a magnetic field are still not clear. Due to the critical role of the mechanical properties on the formability of TWBs, in this work the influences of magnetic treatment on the strength and ductility of TWBs are detected and the mechanism is explained with the combination effect of the magnetic domain and dislocation.

2. Experimental

In this work, the DP600 steel sheet with 1.6 mm in thickness was chosen as the base material of the TWBs. The main parameters of laser welding are shown in Table 1. After the laser welding, a weld seam with a good surface quality, even width (nearly 2 mm) and high straightness is formed.

Table 1. The main parameters of laser welding.

Welding Power/(W)	Welding Speed/(m/s)	Defocusing Amount/(m)	Shielding Gas
1500	0.05	0	Argon

The samples in two different dimensions in length and width were fabricated referred to the Chinese standard GB/228.1-2010 [17] and their sketches are shown in Figure 1. To reduce the measuring error, each group with the same dimension included three non-magnetic treated samples and three magnetic treated ones.

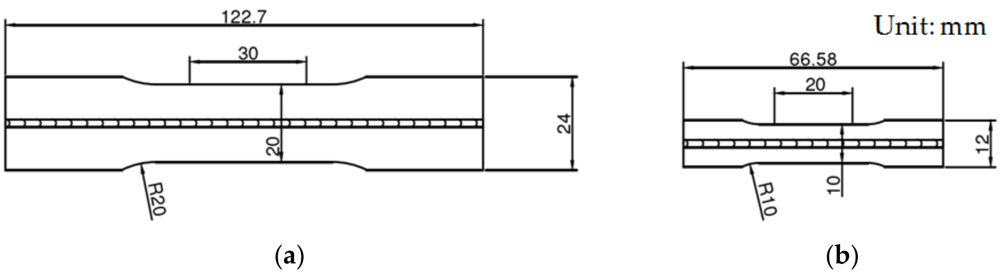

Figure 1. Sketches of the uniaxial tensile test samples with two different dimensions: (**a**) large size; and (**b**) small size.

The magnetic device used here comprises a coil and an AC (Alternating Current) variable frequency power supply, as shown in Figure 2. The inner diameter and height of the coil are about 80 and 201 mm, respectively. The tensile samples were placed in the center of the coil vertically for magnetic treatment. The parameters of magnetic treatment were set as follows: the peak value of magnetic intensity was about 10^4 A/m, the frequency was 50 Hz and the processing time was 90 s. After the magnetic treatment, the mechanical properties of both the non-magnetic treated and magnetic treated samples were measured by a series of uniaxial tensile tests via a material testing machine (Mode: MTS810, MTS, Eden Prairie, MN, USA). All the strain rate used in this work was 0.01/s.

Figure 2. The setup of the magnetic treatment.

3. Results

The broken tensile samples with and without magnetic treatment are shown in Figure 3 and the measured engineering stress–engineering strain curves are given in Figure 4.

(a) (b)

Figure 3. The test samples after uniaxial tensile tests: (**a**) large size; and (**b**) small size.

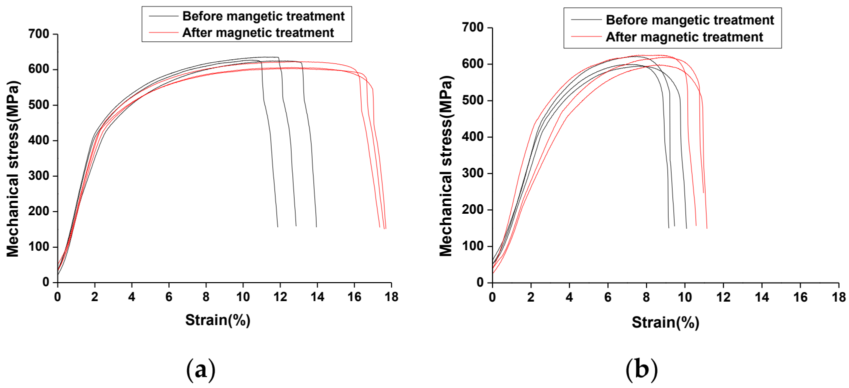

Figure 4. Engineering stress–engineering strain curves before and after magnetic treatments: (**a**) large size; and (**b**) small size.

The mechanical properties including the yield strength, ultimate tensile strength and elongation before and after the magnetic treatment are compared in Figure 5. According to the data in Figure 5a, the average yield strength of TWB samples in both large and small sizes after magnetic treatment increased (or decreased) by less than 5%. Similarly, it can be found from Figure 5b that the average ultimate strength of TWB samples in both large and small sizes after magnetic treatment increased by less than 5%. This indicates that the magnetic treatment has little effect on the strength of the laser TWBs.

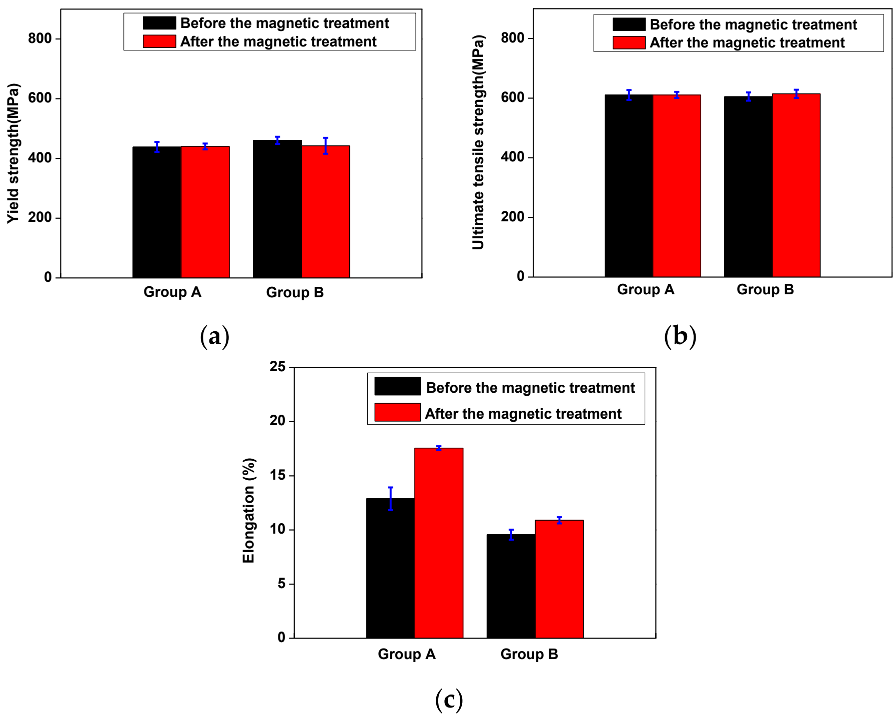

Figure 5. Mechanical properties before and after magnetic treatment: (**a**) yield strength; (**b**) ultimate tensile strength; and (**c**) elongation. Groups A and B represents the samples in large and small sizes, respectively. The blue line segments denote the standard deviation of measured data of three samples in each case.

As can be seen from Figure 5c, however, the average elongations of the samples after the magnetic treatment were increased by 36.23% and 13.90% for the TWB samples in large and small sizes, respectively. The results show that the magnetic treatment can effectively improve the ductility of the laser TWBs.

4. Discussion

Since the plastic deformation is carried out by the movement of dislocations, the change in the mechanical properties of the TWBs after the magnetic treatment can be explained from the evolution of dislocations under a magnetic field. Hence, the dislocations of TWBs before and after magnetic treatment were observed by the transmission electron microscope (TEM, mode: JEM-2100F, JEOL, Tokyo, Japan). Before the TEM test, the thin films with thicknesses of less than 60 μm in the center were obtained by an ion beam thinner for observation.

Figure 6a,b show the microstructures in the FZ of the non-magnetically and magnetically treated TWBs, respectively. As can be seen from the photographs, the microstructure of the FZ was predominantly martensite. The formation of martensite in the FZ was due to the rapid cooling speed of the weld pool during the laser welding process [9]. Before the magnetic treatment, the dislocation density in the FZ was relatively low. After the magnetic treatment, the density of dislocation density increased distinctly with a relatively uniform distribution.

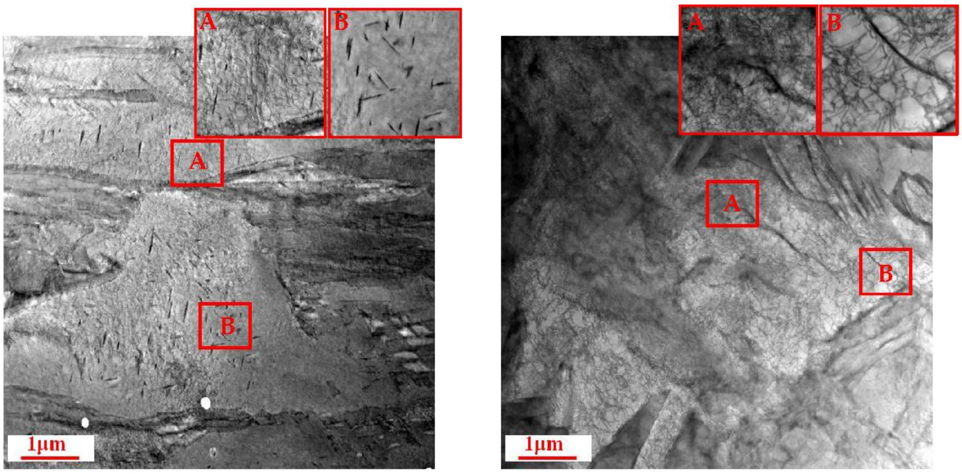

(**a**) (**b**)

Figure 6. Dislocation distribution in the FZ of TWBs: (**a**) before and (**b**) after the magnetic treatment. In order to exhibit the distribution of dislocations, the enlarged images at local positions A and B are shown at the top right corner of each photograph. FZ: fusion zone; TWBs: laser tailor welded blanks.

Figure 7a,b show the microstructures in the HAZ of the non-magnetically and magnetically treated TWBs, respectively. It can be seen that, similar to that of the weld zone, after the magnetic treatment, the dislocation density in the HAZ increased obviously and dislocation nets were formed in some local areas.

The dislocation multiplication after the magnetic treatment is thought to be related to the evolution of magnetic domains for a ferromagnetic material. There are five main interactions in a ferromagnetic material, namely the exchange energy, the magnetocrystalline anisotropy energy, the magnetic and elasticity interaction energy, the demagnetizing field energy and the external magnetic field energy. In order to reduce the demagnetizing energy, self-magnetization magnetic domains are formed in a ferromagnetic material (Figure 8a). Vector $\boldsymbol{M_s}$ is used to represent the average value of the self-magnetization intensity in a single magnetic domain. The directions of $\boldsymbol{M_s}$ in different magnetic domains are disordered before magenization [18]. Therefore, a ferromagnetic material does not exhibit magnetic properties at the macro level without an external magnetic field. Thus the total magnetization intensity of each domain is [19]

$$\sum_i M_s v_i \cos\theta_i = 0 \quad (1)$$

where v_i is the volume of magnetic domain i, θ_i is the angle between $\boldsymbol{M_s}$ and $\boldsymbol{H}$.

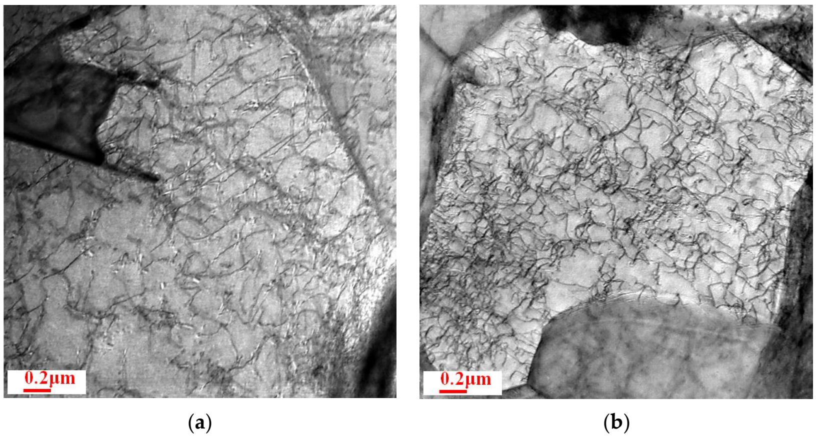

Figure 7. Dislocation distribution in the HAZ of TWBs: (**a**) before and (**b**) after the magnetic treatment. HAZ: heat-affected zone; TWBs: laser tailor welded blanks.

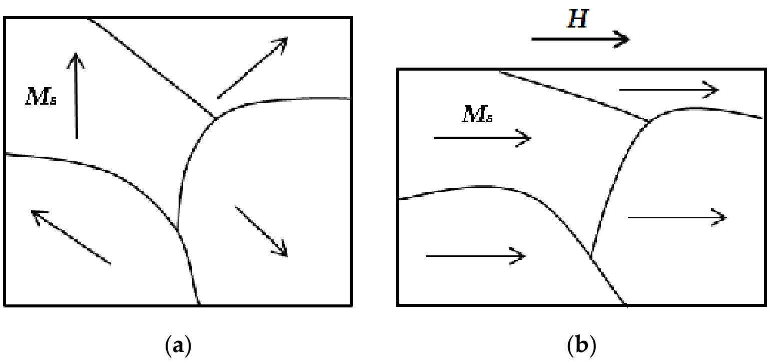

Figure 8. Evolution of magnetic domains: (**a**) before and (**b**) after applying a magnetic field.

When an external magnetic field is applied, the directions of $\boldsymbol{M_s}$ in different magnetic domains become ordered and the ferromagnetic material is then magnetized (Figure 8b). Here, $\boldsymbol{H}$ represents the magnetic field intensity. Then magnetization intensity δM_H along the direction of the external magnetic field can be expressed as follows

$$\delta M_H = \sum_i (M_s \cos\theta_i \delta v_i - M_s v_i \sin\theta_i \delta\theta_i + v_i \cos\theta_i \delta M_s) \quad (2)$$

where the expression $M_s \cos\theta_i \delta v_i$ is related to the movement of domain walls due to the growth of magnetic domains. The expression $M_s v_i \sin\theta_i \delta\theta_i$ is related to the change of the direction of the vector M_s due to the rotation of the magnetic domains. The expression $v_i \cos\theta_i \delta M_s$ is related to the increase of vector M_s. The evolution of the magnetic domains in a ferromagnetic material will certainly cause local stress. For example, the stress caused by the movement of domain walls in a local area was deduced in our former work [20] and can be expressed by

$$\sigma_i \approx \frac{2}{3\lambda_s A_1}(\mu_0 H M_s x \times \cos\theta + C)^2 - \frac{2K_1}{3\lambda_s} \quad (3)$$

The above stress further causes local strain and micro-deformations in the ferromagnetic material and thus contributes to the multiplication of dislocations.

Based on the above, the increase of the dislocation density in TWBs after magnetic treatment can be illustrated by the mechanism of Frank-Read dislocation multiplication. In Figure 9a, DD′ is a dislocation line and it cannot move because of its two fixed endpoints and the obstacles may be a fixed dislocation, impurities or foreign particles, and so on. When the external magnetic field is applied, the component of stress, τ, starts to act on the dislocation line DD′. Due to the fixed nodes D and D′, the line dislocation DD′ can only bend forward, as shown in Figure 9b. Once the dislocation line bends to more than a semicircle, it curls and forms helical branches m and n around D and D′, as shown in Figure 9c,d. When the two bending lines gradually approach, helical branches m and n, whose Burgers vectors, ***b***, are opposite, annihilate after meeting. Thus the dislocation line is divided into two parts, as shown in Figure 9e. After that, the dislocation DD′ goes back to its original position and repeats the above process and finally results in the increase of the dislocation density [21,22].

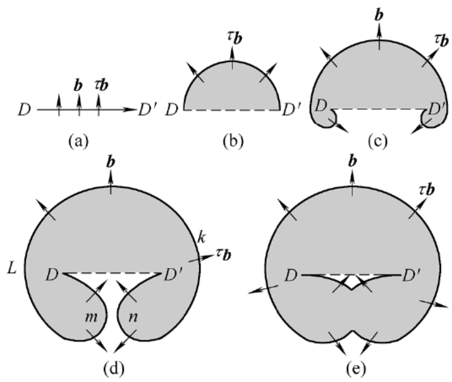

Figure 9. Frank-Read dislocation multiplication [22]: (**a**)–(**e**) the process of dislocation multiplication. In the figure, ***b*** is the Burgers vector and τ is the component of stress applied on the dislocation line DD′ under a magnetic field.

The increase of the dislocation density is the main cause of the ductility improvement of the TWBs. The mechanism is deduced by the relationship model between the dislocation and shear strain as shown in Figure 10. Using b to represent the value of Burgers vector ***b***, when the dislocation moves through an element in a unit length along the slip plane, the shear strain can be expressed as [23]

$$\gamma = \frac{b}{h} \tag{4}$$

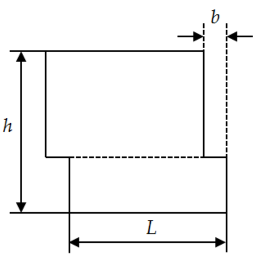

Figure 10. Relationship model between dislocation and shear strain. *b*: the value of Burgers vector ***b***; *h:* the width of element; *L*: the length of element.

Assuming that the dislocation slip distance is x_i, and the displacement at the top of the element, relative to its bottom, is

$$\delta_i = \frac{x_i b}{L} \tag{5}$$

The total displacement produced by the slip of N dislocations on many parallel slip planes is

$$\Delta = \sum_{i=1}^{N} \delta_i = \frac{b}{L} \sum_{i=1}^{N} x_i \tag{6}$$

The corresponding shear strain is

$$\gamma = \frac{\Delta}{h} = \frac{b}{hL} \sum_{i=1}^{N} x_i \tag{7}$$

The average displacement of dislocations $\overline{x}$ can be expressed as

$$\overline{x} = \frac{1}{N} \sum_{i=1}^{N} x_i \tag{8}$$

Then the shear strain caused by the slip of N dislocations on a series of parallel slip planes is

$$\gamma = \frac{bN\overline{x}}{hL} = b\rho\overline{x} \tag{9}$$

Thus, the average displacement of the dislocations can be further written as

$$\overline{x} = \frac{\gamma}{b\rho} \tag{10}$$

where $\rho = N/(hL)$ is the dislocation density.

Considering the plastic deformation at a certain moment of the uniaxial tensile test, the average displacements of dislocations at the beginning and end of the deformation are supposed to be $\overline{x_0}$ and $\overline{x_b}$, respectively. According to Equation (10), different dislocation density values bring different line slopes and shear strains in Figure 11. Therefore, a higher dislocation density causes a smaller slope and thus a larger shear strain, i.e., $\gamma_t > \gamma_u$. Since the dislocation density of the magnetically treated TWBs is much higher than that of non-magnetically treated ones according to the results of TEM, the former has a much larger strain for a certain average displacement of dislocations. The displacement, in the plastic deformation process, is continuous from the beginning to the fracture of the TWB. Namely, the process of the dislocation slip is continuous. Therefore, it can be concluded that the magnetically treated TWBs have a higher elongation.

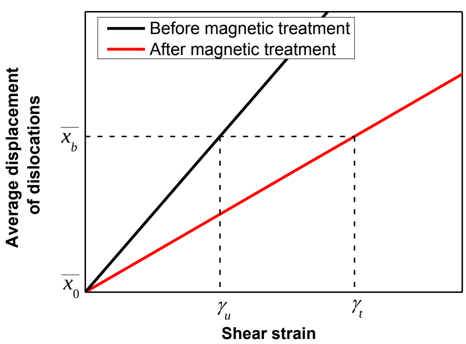

Figure 11. Relationship between average displacement of dislocations $\overline{x}$ and shear strain γ.

The increase of the dislocation density leads to the formation of dislocation cells, which further affects the local stress/strain field and thus the ductility of TWBs. At the same time, the evolution of the magnetic domain under the magnetic field and the dimensions of the uniaxial tensile samples also increase the complexity of magnetic treatment effects on TWBs.

5. Conclusions

(1) The yield strengths and the ultimate tensile strength of the TWBs changed slightly (less than 5%), but the elongation increased by 13.90%–36.23% after the magnetic treatment.

(2) The increase in the elongation of laser TWBs is mainly caused by the increase of the dislocation density, which is explained by the relationship model between the dislocation and shear strain.

(3) The evolution of the magnetic domain of ferromagnetic materials under the magnetic field produces local stress and strain, which can promote the multiplication of dislocations.

(4) The comprehensive effect of the magnetic domain evolution, the dislocation evolution and the corresponding changes in the stress/strain field increases the complexity of property changes under the magnetic field.

Acknowledgments: This work is supported by the National Natural Science Foundation of China (Grant Nos. 51305317 and 51675392), the Natural Science Foundation of Hubei Province of China (Grant No. 2014CFA119) and the Special Project of Technological Innovation of Hubei Province (Grant No. 2016AAA053). The authors would also like to acknowledge the MatProFuture Project.

Author Contributions: Yanli Song determined the idea, methods and structure of the paper and revised the manuscript. Hailong Yu and Chenyu Zhao performed the uniaxial tensile experiments; Cheng Yu performed the TEM experiment, analyzed the data and wrote the manuscript.

Conflicts of Interest: The authors declare no conflict of interest.

References

1. Schrek, A.; Švec, P.; Gajdošová, V. Deformation properties of tailor welded blank made of dual phase steels. *Acta Mech. Autom.* **2016**, *10*, 38–42. [CrossRef]
2. Song, Y.L.; Hua, L.; Meng, F.Z. Inhomogeneous constructive modelling of laser welded bead based on nanoindentation test. *Ironmak. Steelmak.* **2012**, *39*, 95–103. [CrossRef]
3. Song, Y.L.; Hua, L.; Chu, D.N.; Lan, J. Characterization of the inhomogeneous constitutive properties of laser welding beams by the micro-Vickers hardness test and the rule of mixture. *Mater. Design* **2012**, *37*, 19–27. [CrossRef]
4. Padmanabhan, R.; Oliveira, M.C.; Menezes, L.F. Deep drawing of aluminium-steel tailor-welded blanks. *Mater. Design.* **2008**, *29*, 154–160. [CrossRef]
5. Meinders, T.; Berg, A.V.D.; Huétink, J. Deep drawing simulations of tailored blanks and experimental verification. *J. Mater. Process. Technol.* **2000**, *103*, 65–73. [CrossRef]
6. Lee, W.; Chung, K.H.; Kim, D.; Kim, J.; Kim, C.; Okamoto, K.; Wagoner, R.H.; Chung, K. Experimental and numerical study on formability of friction stir welded TWB sheets based on hemispherical dome stretch tests. *Int. J. Plast.* **2009**, *25*, 1626–1654. [CrossRef]
7. Sinha, A.K.; Kim, D.Y.; Ceglarek, D. Correlation analysis of the variation of weld seam and tensile strength in laser welding of galvanized steel. *Opt. Lasers Eng.* **2013**, *51*, 1143–1152. [CrossRef]
8. Song, Y.L.; Hua, L. Influence of inhomogeneous constitutive properties of weld materials on formability of tailor welded blanks. *Mater. Sci. Eng. A* **2012**, *552*, 222–229. [CrossRef]
9. Farabi, N.; Chen, D.L.; Li, J.; Zhou, Y.; Dong, S.J. Microstructure and mechanical properties of laser welded DP600 steel joints. *Mater. Sci. Eng. A* **2010**, *527*, 1215–1222. [CrossRef]
10. Kang, C.Y. Characteristics of Nd:YAG laser welded 600 MPa grade TRIP and DP steels. *Mater. Sci. Forum* **2007**, *539*, 3967–3972. [CrossRef]
11. Lu, A.L.; Tang, F.; Luo, X.; Mei, J.; Fang, F. A new method for residual stress reduction—Pulsed magnetic treatment. *China Mech. Eng.* **1998**, *9*, 40–42.
12. Zhao, W.X.; Yao, H.M.; Liang, Z.Q. Effect of pulsed magnetic field on the micro-hardness of HSS cutting tool materials. *Trans. Beijing Inst. Technol.* **2014**, *34*, 661–665.

13. Celik, A.; Yetim, A.F.; Alsaran, A.; Karakan, M. Effect of magnetic treatment on fatigue life of AISI 4140 steel. *Mater. Design* **2005**, *26*, 700–704. [CrossRef]
14. Klamechi, B.E. Residual stress reduction by pulsed magnetic treatment. *J. Mater. Process. Technol.* **2003**, *141*, 385–394. [CrossRef]
15. Cai, Z.P.; Lin, J.; Zhao, H.Y.; Lu, A.L. Orientation effects in pulsed magnetic field treatment. *Mater. Sci. Eng. A* **2005**, *398*, 344–348.
16. Song, Y.L.; Hua, L. Mechanism of residual stress reduction in low alloy steel by a low frequency alternating magnetic treatment. *J. Mater. Process. Technol.* **2012**, *28*, 803–808. [CrossRef]
17. Standardization Administration of the People's Republic of China. *Metallic Materials-Tensile Testing—Part 1: Method of Test at Room Temperature*; GB/228.1-2010; Standardization Administration of the People's Republic of China: Beijing, China, 2010.
18. Geng, G.H. *Materials Physics and Properties*; Peking University Press: Beijing, China, 2010; pp. 238–267.
19. Jiang, S.T. *Condensed Magnetic Physics*; Science Press: Beijing, China, 2003; pp. 378–420.
20. Song, Y.L. Transition in Structure and Properties of Ferromagnetic Materials Caused by a Low Frequency Alternating Magnetic Field. Master Thesis, Wuhan University of Technology, Wuhan, China, 13 December 2008.
21. Hu, G.X. *Metallography*; Shanghai Scientific & Technical Publishers: Shanghai, China, 1980; pp. 63–107.
22. Wang, Y.N.; Chen, S.J.; Dong, X.C. *Dislocation Theory and Its Applications*; Metallurgical Industry Press: Beijing, China, 2007; pp. 62–75.
23. Yang, D.Z. *Dislocation and Metal Strengthening Mechanism*; Harbin Institute of Technology Press: Harbin, Chain, 1991; pp. 107–134.